PHYS 4350 – Tracking Module

Spacecraft Tracking and Deep Space Antenna Calibration Measurements

Arvin Tangestanian - 214195796

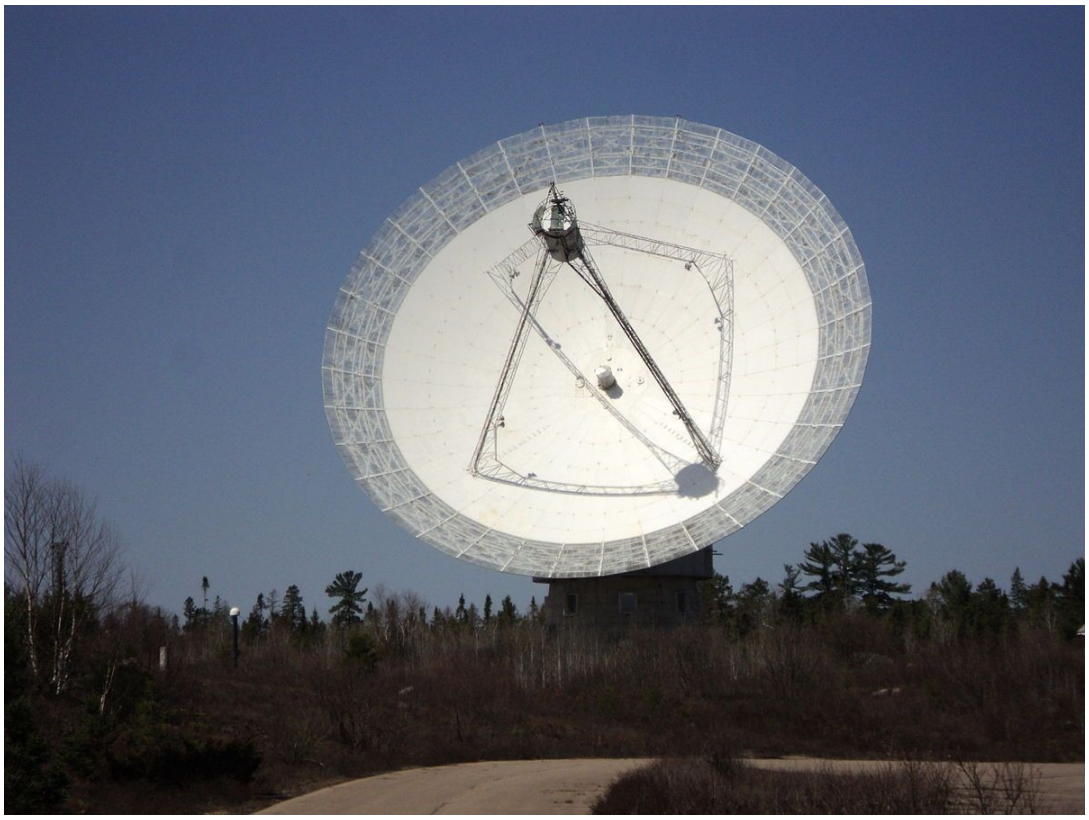

Arvin Tangestanian

Experiment Date: 1st May 2019

Table of Contents

1.0 Purpose

The goal of the tracking module was to create a software package to point an antenna at a GPS satellite and receive a down link signal. The software was developed over a five week period, and tested at the Algonquin Radio Observatory Facility. The software had to be able to propagate satellite trajectories from TLE epoch up to and through any given observation time interval, and calculate the azimuth and elevation look angles from the facility to the satellite. The software should also calculate the access times and minimum received power at facility for each GPS satellite.

The purpose of this software project was to test the groups understanding of RF communication, orbital mechanics, and other concepts studied in the course. Additionally, testing at ARO provides experience with This software project also provided an opportunity to apply these concepts to a practical situation, and give experience with programming, debugging, and working with real hardware systems. The software was developed using Python 3, for the front-end input/output, and OpenModelica for the back-end simulation.

The software was developed over a period of about 6 weeks, in three distinct stages. The first stage (weeks P1 and P2) consisted of creating the basic simulation model in OpenModelica and some of the Python functions necessary for the task. The second stage (weeks P3, P4, P5) consisted of completing the higher level simulation models and the remaining Python functions, as well as integrating the different modules. The third stage, from post P5 to the day of software testing, consisted of debugging, integration, and field testing. Software testing was performed throughout the process, using resources like STK to verify results.

The software development is described in detail within the previous lab reports. This report will focus on the performance of the completed software package during the experiments conducted at ARO.

2.0 Results

2.1 Activity 1, ARO Dish Antenna Pattern

There were three main activities to be performed at the Algonquin Radio Observatory. The first activity was to measure the antenna radiation pattern for the 46 meter dish. This radiation pattern is a measure of how the received power levels are affected by azimuth or elevation offsets. This measurement activity was performed in a large group, with team (Arvin, Tiffany), as well as team 4 (David, Constantine), team 5 (Rafi, Matthieu), and team 7 (Sogand,Gabirel). These measurements will also determine the atmospheric attenuation and system gain.

First, a facility technician used the ARO in-house software package to select a GPS satellite and track it with the dish. The satellite tracked was PRN 22. Next, the spectrum analyzer was adjusted to view the signal properly. The spectrum analyzer was controlled remotely, using a LabView interface. Based on the AOS/LOS table computed by our software package, it was estimated that the received power would be at about -66 dBm. It was known that the RF signal would have a centre frequency of 1.575 GHz. Based on these parameters, the group agreed to set the spectrum analyzer to the settings shown in **Table 1**.

Table 1 Spectrum Analyzer Settings for Radiation Pattern Measurements

Spectrum Analyzer Parameter	Value
RBW	49.602 kHz
VBW	10.000 kHz
Averaging	100
Reference Power Level	-50 dBm

After the ARO technician initiated the tracking sequence, there was a brief waiting period as the antenna moved to the correct look angles. Once the dish was in position, the facility display monitor indicated “on track”, and the following frequency spectrum was observed (**Figure 1**). **Figure 2** shows the ARO display monitor indicating the dish look angles and tracking status. The peak search function was used to place a marker at the peak.

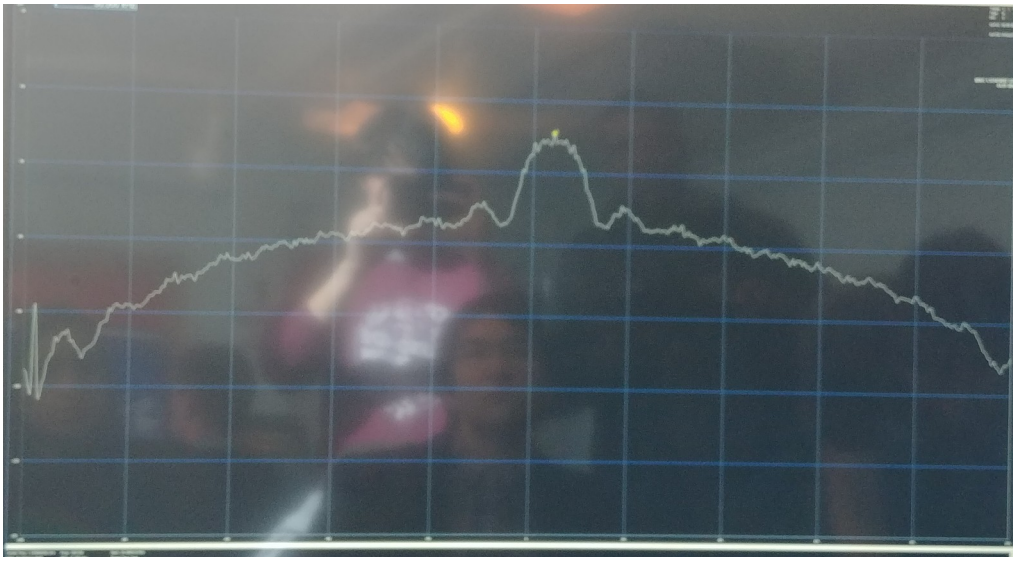

Figure 1: *Signal received from PRN 22 during radiation pattern measurements*

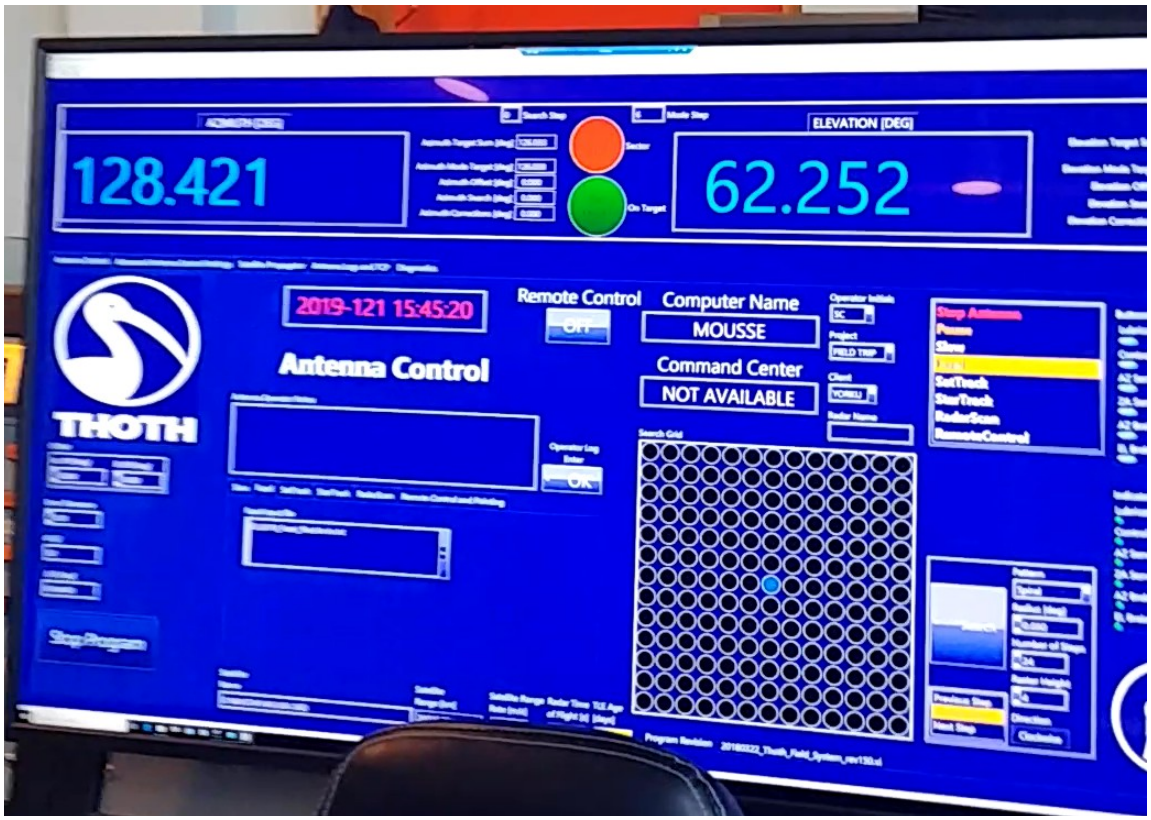

Figure 2: *ARO in-house tracking software. This display indicates the tracking status, as well as the current dish look angles. It should be noted that during this activity, PRN-22 was at an elevation of around 60 degrees, decreasing steadily.*

Once the dish was on target and it was confirmed that the spectrum analyzer settings were satisfactory, the technician asked the group what angular offset to use for the measurements. The group chose to measure in 0.1° increments, taking ten measurements on each side (**Section 4.0 Discussion** will explore this in further detail). The elevation radiation pattern was measured first. The azimuth offset was maintained at 0 for these measurements. For each of these measurements, first the technician would announce his change in offset, then the group would wait for the dish to re-align, and also wait a few more moments for the spectrum analyzer averaging feature to work through. The group recorded the peak power level at each of these angular offsets. The offsets started at +0.1° and went up to +1.0°, and then re-adjusted to zero and went down to -1.0°. The data is presented in **Table 2** below. It should be noted that the power levels were changing on the order of about ~0.2 dBm every second, and as such the observations recorded represent an eyeball estimate of the most common values seen. A scatter plot of this radiation pattern is shown in **Figure 11**.

Table 2: Elevation Radiation Pattern Measurements for ARO Dish

Elevation Offset [deg]	Peak Power [dBm]
1	-97.01
0.9	-91.14
0.8	-89.77
0.7	-96.8
0.6	-85.55
0.5	-87.2
0.4	-82.6
0.3	-79.8
0.2	-78.7
0.1	-69.5
0	-64.4
-0.1	-64.3
-0.2	-67.67
-0.3	-73.45
-0.4	-77.36
-0.5	-82.7
-0.6	-97.21
-0.7	-94.12
-0.8	-97.56
-0.9	-88.17
-1	-89.7

Once the elevation measurements were complete, the process was repeated for the azimuth radiation pattern. For these measurements, the elevation offset was kept at a constant -0.1° as the azimuth was stepped through in increments of 0.1°. The measurements are presented in **Table 3**, and a scatter plot of the points are in **Figure 12**.

Table 3: Azimuth Radiation Pattern Measurements for ARO Dish, with ΔEl = -0.1°

Azimuth Offset [deg]	Peak Power [dBm
1	-89.22
0.9	-96.38
0.8	-92.61
0.7	-89.17
0.6	-92.19
0.5	-82.57
0.4	-78.81
0.3	-74.35
0.2	-68.11
0.1	-64.7
0	-64.61
-0.1	-65.78
-0.2	-70.44
-0.3	-75.32
-0.4	-79.46
-0.5	-86.19
-0.6	-88.94
-0.7	-86.65
-0.8	-95.62
-0.9	-92.12
-1	-88.24

It should be noted that at this point, between activities 1 and 2, the tracking software was modified slightly. Using the results from the first activity, the code was updated to accurately model the atmospheric attenuation and system gain. This will be explored in the discussion section.

2.2 Activity 2, Spacecraft Tracking and Software Delivery

The second activity was to use the team software package to produce a pointing file and track a GPS operational satellite. Prior to the activity, the TLE file used by the code was updated to use the most recent set from CelesTrak. This experiment began by presenting the SatTrak package to professor Chesser. The code was initiated by running the main script through Spyder, a Python IDE. This activity was performed on May 1st 2019, at around 11:40 AM local time. The Professor selected the current day, and requested a tracking interval from 15:45:00 to 16:15:00 UTC, in 5 second increments. The software ran as expected, and after a few moments presented the AOS/LOS table to the user. A screenshot of this output is shown in **Figure 3**.

```
Computed from 01 May 2019 15:45:00.000000 to 01 May 2019 16:14:59.999999 with timestep = 5 seconds

 # |   Satellite Name              |   AOS                          |   LOS                          |   Min. Power [dBm]

 1 |   GPS BIIA-23 (PRN 18)        |   None                         |   None                         |        -69.990128
 2 |   GPS BIIR-2  (PRN 13)        |   None                         |   None                         |        -70.662509
 3 |   GPS BIIR-3  (PRN 11)        |   None                         |   None                         |        -69.857440
 4 |   GPS BIIR-4  (PRN 20)        |   None                         |   None                         |        -70.517706
 5 |   GPS BIIR-5  (PRN 28)        |   None                         |   None                         |        -70.053086
 6 |   GPS BIIR-6  (PRN 14)        |   None                         |   None                         |        -70.784342
 7 |   GPS BIIR-8  (PRN 16)        |   01 May 2019 15:45:00.000000  |   01 May 2019 16:14:59.999999  |        -68.122719
 8 |   GPS BIIR-9  (PRN 21)        |   01 May 2019 15:45:00.000000  |   01 May 2019 16:14:59.999999  |        -69.406872
 9 |   GPS BIIR-10 (PRN 22)        |   None                         |   None                         |        -70.300640
10 |   GPS BIIR-11 (PRN 19)        |   None                         |   None                         |        -71.477828
11 |   GPS BIIR-12 (PRN 23)        |   01 May 2019 15:45:00.000000  |   01 May 2019 16:14:59.999999  |        -68.294590
12 |   GPS BIIR-13 (PRN 02)        |   None                         |   None                         |        -70.907321
13 |   GPS BIIRM-1 (PRN 17)        |   None                         |   None                         |        -71.027530
14 |   GPS BIIRM-2 (PRN 31)        |   None                         |   None                         |        -70.117949
15 |   GPS BIIRM-3 (PRN 12)        |   None                         |   None                         |        -71.719928
16 |   GPS BIIRM-4 (PRN 15)        |   None                         |   None                         |        -71.108755
17 |   GPS BIIRM-5 (PRN 29)        |   None                         |   None                         |        -70.773193
18 |   GPS BIIRM-6 (PRN 07)        |   01 May 2019 15:45:00.000000  |   01 May 2019 16:14:59.999999  |        -68.347913
19 |   GPS BIIRM-8 (PRN 05)        |   None                         |   None                         |        -69.518736
20 |   GPS BIIF-1  (PRN 25)        |   None                         |   None                         |        -71.401942
21 |   GPS BIIF-2  (PRN 01)        |   None                         |   None                         |        -70.373918
22 |   GPS BIIF-3  (PRN 24)        |   None                         |   None                         |        -71.702235
23 |   GPS BIIF-4  (PRN 27)        |   01 May 2019 15:45:00.000000  |   01 May 2019 16:14:59.999999  |        -67.610452
24 |   GPS BIIF-5  (PRN 30)        |   01 May 2019 15:51:11.498102  |   01 May 2019 16:14:59.999999  |        -69.355142
25 |   GPS BIIF-6  (PRN 06)        |   None                         |   None                         |        -71.043108
26 |   GPS BIIF-7  (PRN 09)        |   01 May 2019 15:45:00.000000  |   01 May 2019 16:14:59.999999  |        -67.974946
27 |   GPS BIIF-8  (PRN 03)        |   None                         |   None                         |        -70.259593
28 |   GPS BIIF-9  (PRN 26)        |   01 May 2019 15:45:00.000000  |   01 May 2019 16:14:59.999999  |        -69.028073
29 |   GPS BIIF-10  (PRN 08)       |   01 May 2019 15:45:00.000000  |   01 May 2019 16:14:59.999999  |        -68.097470
30 |   GPS BIIF-11  (PRN 10)       |   None                         |   None                         |        -70.772217
31 |   GPS BIIF-12  (PRN 32)       |   None                         |   None                         |        -71.124007

Press Enter to Continue:

Please Select Which Satellite To Track: 11
##Writing Pointing File for  GPS BIIR-12 (PRN 23)
...
##COMPLETE
```

Figure 3: *AOS/LOS table presented to the user during the experiment*

As seen at the lower portion of the figure above, the user was prompted to select a satellite for tracking. Professor Chesser decided to track PRN 23. The package then printed the pointing information to a file titled “pointing.txt”. **Figure 4** shows the first few lines of this file. At this point the pointing file was transferred to the facility computer system. A direction connection was not permitted, so there was a momentary delay as an internet connection was established and the file was emailed to the technician. The pointing file was loaded into the facility tracking system using the FAZL reader. The file was read succesfully and the dish moved into position to track the satellite.

```
#Pointing File For  GPS BIIR-12  (PRN 23)
2019.121.15:45:00 126 25 26.1  0.002 62  8 50.6  0.102
2019.121.15:45:04 126 20 45.4  0.002 62 10 12.4  0.101
2019.121.15:45:10 126 16  4.2  0.002 62 11 34.0  0.101
2019.121.15:45:15 126 11 22.5  0.002 62 12 55.4  0.100
2019.121.15:45:19 126  6 40.3  0.002 62 14 16.6  0.100
2019.121.15:45:24 126  1 57.6  0.002 62 15 37.6  0.100
2019.121.15:45:30 125 57 14.4  0.002 62 16 58.3  0.099
2019.121.15:45:35 125 52 30.8  0.002 62 18 18.8  0.099
2019.121.15:45:39 125 47 46.6  0.002 62 19 39.1  0.099
```

Figure 4: *Sample of pointing file used during tracking*

The spectrum analyzer was operated remotely using a LabView module. The settings were adjusted to match the same values as in activity 1 (see **Table 1** for the settings used). After a few moments of waiting for the dish to align, the frequency spectrum in **Figure 5** was observed.

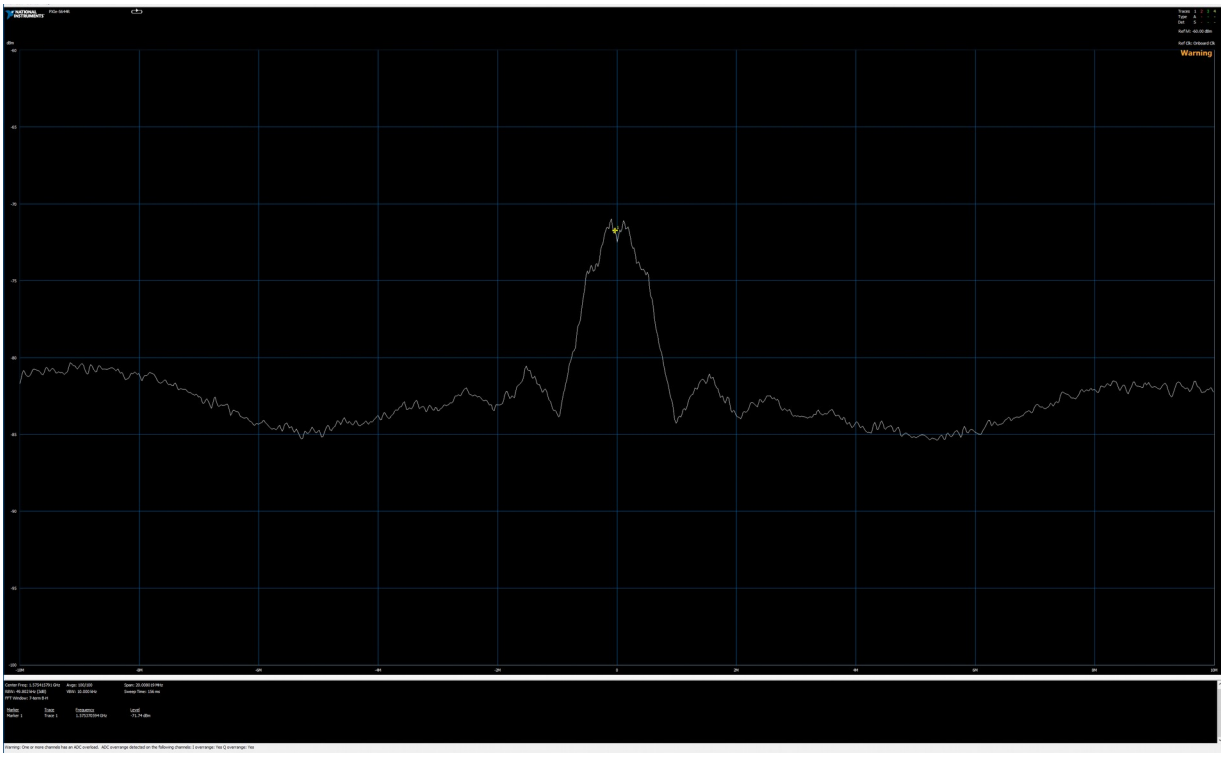

Figure 5: Received *power from PRN-23, tracking using the developed software package*

The peak power level was measured to be at about -71.74 dBm. As seen in **Figure 3** above, the software computed a minimum power of -68.29 dBm.

2.3 Activity 3, Mystery TLE

The third and final activity involved tracking an unknown GPS satellite. First, the team was given a new TLE file containing 68 “mystery” satellites. This TLE file was fed into the software package. The software was run again, for the date May 1st 2019, and time interval 16:25:00 to 17:30:00 UTC with a time step of 5 seconds. The code took slightly longer to operate than it did for the initial 31 satellite file, but after a few moments of waiting it provided the user with the AOS/LOS table, **Figure 6**.

AOS/LOS Table for ARO Facility.
Computed from 01 May 2019 16:24:59.999999 to 01 May 2019 17:30:00.000000 with timestep = 5 seconds

#	Satellite Name	AOS	LOS	Min. Power [dBm]
1	MYSTERY 1	None	None	-70.386317
2	MYSTERY 2	None	None	-71.238826
3	MYSTERY 3	None	None	-70.293301
4	MYSTERY 4	01 May 2019 16:24:59.999999	01 May 2019 17:30:00.000000	-68.268722
5	MYSTERY 5	01 May 2019 16:24:59.999999	01 May 2019 17:30:00.000000	-67.447984
6	MYSTERY 6	None	None	-70.331987
7	MYSTERY 7	None	None	-70.723016
8	MYSTERY 8	None	None	-74.616075
9	MYSTERY 9	01 May 2019 16:24:59.999999	01 May 2019 17:30:00.000000	-67.533973
10	MYSTERY A	None	None	-70.309192
11	MYSTERY B	01 May 2019 16:35:33.420659	01 May 2019 17:30:00.000000	-69.041884
12	MYSTERY C	None	None	-74.695239
13	MYSTERY D	None	None	-74.303217
14	MYSTERY E	None	None	-71.360230
15	MYSTERY F	None	None	-74.401818
16	MYSTERY G	None	None	-75.011199
17	MYSTERY H	None	None	-74.633582
18	MYSTERY J	None	None	-74.660242
19	MYSTERY K	None	None	-75.044173
20	MYSTERY L	01 May 2019 16:24:59.999999	01 May 2019 17:30:00.000000	-69.863529
21	MYSTERY M	None	None	-71.165048
22	MYSTERY N	01 May 2019 16:24:59.999999	01 May 2019 17:30:00.000000	-68.780377
23	MYSTERY O	None	None	-70.866751
24	MYSTERY P	None	None	-70.630962
25	MYSTERY Q	None	None	-74.544150
26	MYSTERY R	None	None	-70.792948
27	MYSTERY S	None	None	-71.953387
28	MYSTERY T	None	None	-70.962487
29	MYSTERY U	None	None	-71.410517
30	MYSTERY V	01 May 2019 17:20:07.687740	01 May 2019 17:30:00.000000	-70.581113
67	MYSTERY 1W	01 May 2019 16:24:59.999999	01 May 2019 17:30:00.000000	-68.584295

Figure 6: *AOS/LOS table printed for the mystery tracking exercise. Note that the full table is not displayed as it is too large. The first 30 satellites are displayed, as well as the satellite chosen for tracking.*

Satellite 1W was chosen for tracking, and a pointing file was generated. As explained for the previous activity, the pointing file was loaded into the ARO facility computer system. The file was read successfully and the dish moved into position. Initially, the spectrum analyzer was set to the same settings as in activity 1 (**Table 1**). Once the dish was on target and a signal was observed, the span, reference power, and centre frequency were adjusted to get a good image of the signal. **Figure 7** shows the signal received from the mystery satellite, as well as the new settings.

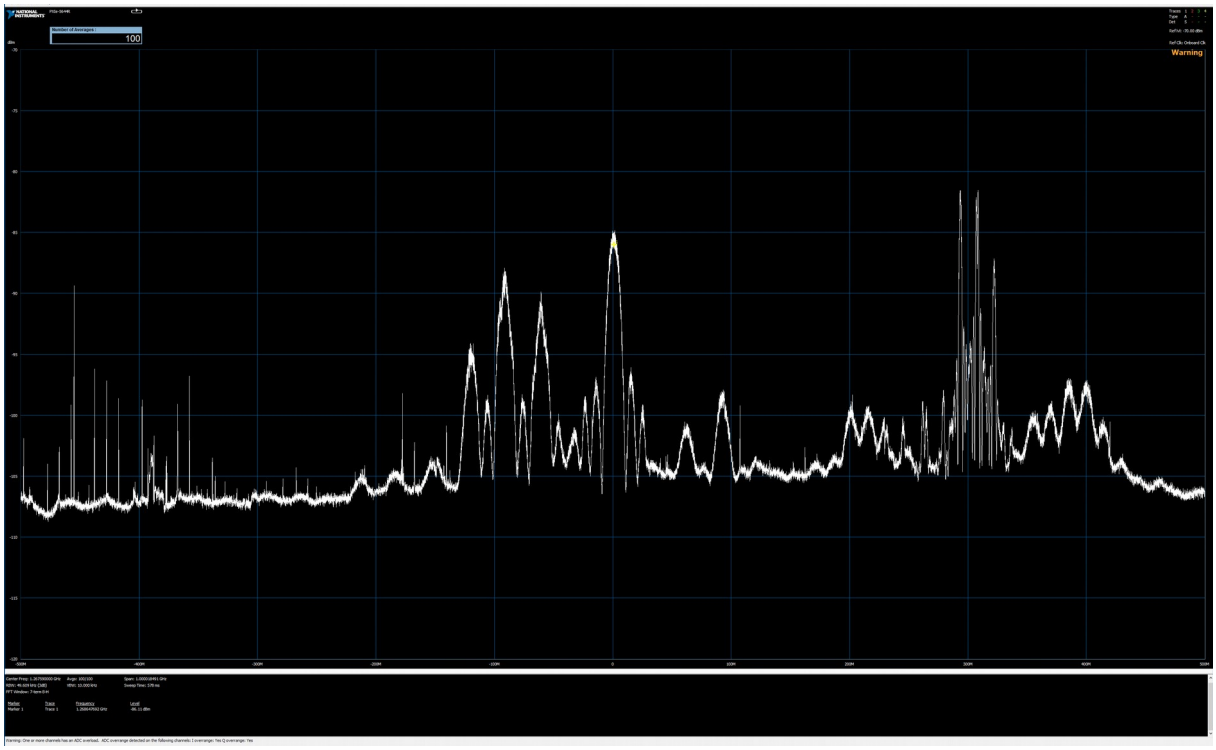

Figure 7: Received *power from the mystery satellite. Note the cluster of peaks centred around 1.2686 GHz (middle) and the narrower cluster of peaks centred around ~300 M, 1.5686 GHz (right)*

Note that the figure above was recorded to observe the entire spectrum. However during the activity, the signal was investigated very thoroughly by changing the centre frequencies and spans to observe each of the activate frequency components. After viewing the signal and considering the positions of the peaks, the team deduced that we were looking at a BEIDOU operational satellite (this thought process is explored in the discussion section). We told this final answer to the technician, and were informed that we were correct in our deduction. We were informed that the mystery satellite 1W corresponded to BEIDOU-3, NORAD number 43707.

3.0 Discussion & Interpretation

3.1 Activity 1, ARO Dish Antenna Pattern

3.1.1 Antenna Theory

During this activity, it was required to select an increment for the angle offsets. It is known that for this dish, the half power beam width (HPBW) is 0.3 degrees. As seen in **Figure 8** below, HPBW corresponds to the width of the -3 dB band. The bandwidth first null, BWFN (labelled as FNBW in the diagram) and first side lobe occur at angular distances slightly beyond HPBW. This figure shall be used as a reference when interpreting the results of our measurements.

The group decided that in order to properly measure the radiation pattern, we would need to observe all of these key features. Of course, it was necessary for the increment to be less than 0.3 degrees, otherwise the resolution would be too vague to pick up any of these details. But on the other hand, an increment too small would take a long time to record. I personally wanted to measure in increments of 0.05 degrees, as I felt that this would be a good balance between resolution and time management, but the group voted against this and decided for 0.1 degrees instead. It was decided to take 10 measurements on each side (going up to +1°), because as approximately three times the HPBW we can expect to see up to at least the first side lobe.

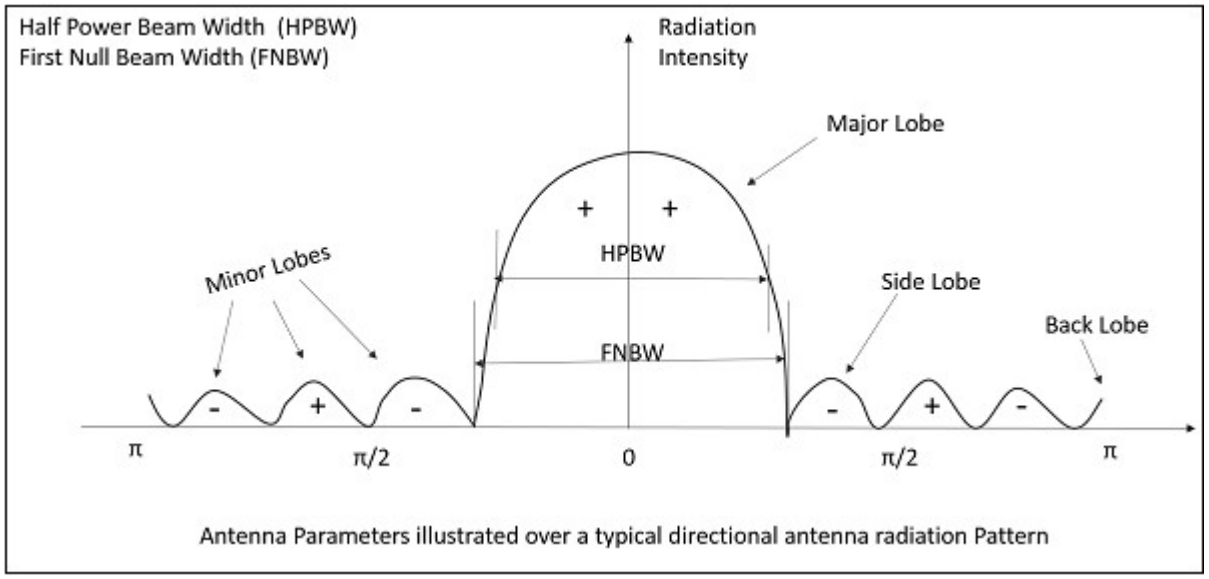

Figure 8: *Illustration of a typical radiation pattern, with key features labelled.* **[1]**

4.1.2 Fluctuating Power Levels

As noted previously, the power readings were fluctuating constantly in the order of about 0.2 dBm each second. This can be due to a few reasons. The largest factor affecting a change in the power reading will be the distance between the dish and the satellite. Since the satellite is travelling at an orbital velocity of about 3.8 km/s the range is changing considerably, on the order of about . Additionally, the elevation angle of the satellite is also changing at each second (although at a much slower rate). **Figure 9** is a plot of the range from ARO to Satellite for PRN 18 over two minutes at a generic time interval, demonstrating a rate of change of about 439 metres per second. Additionally, the weather conditions were not optimal during the tracking period as it was very cloudy. The dynamic atmospheric attenuation due to water particles in the clouds and other environmental factors will also contribute to changing power levels. The final factor contributing to this unsteady power reading is the changing elevation angle as the satellite moves across the sky. As discussed in class, the GPS transmitters actually perform better at mid elevation angles of about 40 degrees (**Figure 10**). Elevations tending towards 0 or 90 degrees diminish the power by about 3 degrees.

Realistically, each of these factors alone are virtually insignificant, especially for the purposes of this activity. But when combined they are a considerable element that can affect precise experiments such as radio astronomy.

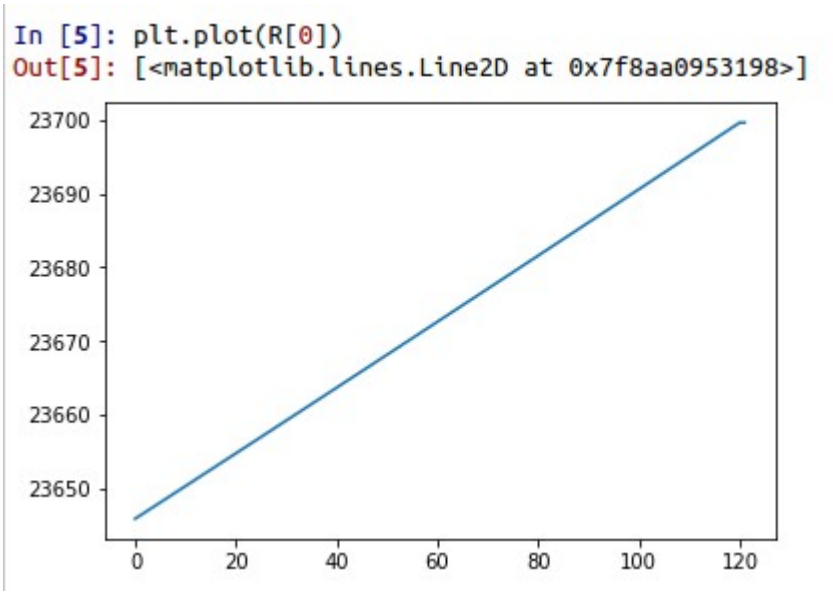

Figure 9: *Python plot of a generic satellite range changing over time. This data computed for PRN 18 to ARO, May 9th 2019 from 10:00:00 to 10:02:00 UTC with a two second time step.*

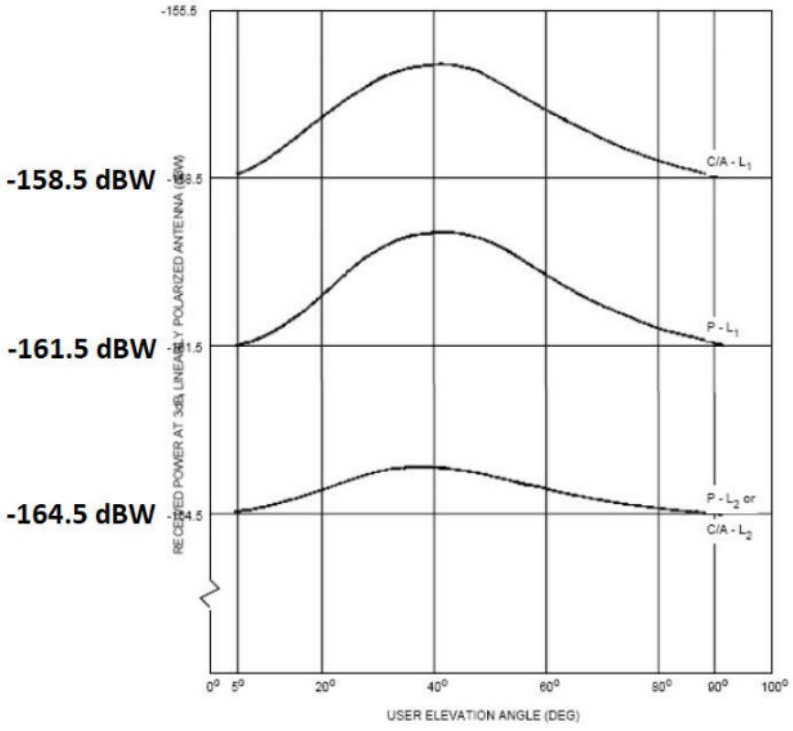

Figure 10: *Plot of different GPS received power levels over different elevations* **[2]**

3.1.3 Elevation Antenna Radiation Pattern

The measurements recorded for the elevation radiation pattern (**Table 2)** are presented in **Figure 11** below. The data for the azimuth radiation pattern (**Table 3**) is in **Figure 12**. It is at first apparent that the elevation plot is not symmetrical, and does not demonstrate the typical shape we expect from **Figure 8**. This may be due in part to the inaccuracy of the recorded data (writing down a typical value for a number that is changing every second). In particular, the region between 0 and 0.6 degrees appear to be “squished”. It may be worth noting that these were the first six measurements, and it is entirely possible that these measurements were rushed or recorded inaccurately.

Even with the asymmetry present, the key features of a radiation pattern are observable. Since the peak is at -64.3 dBm, we will measure the HPBW at -67.3 dBm. Checking the data in **Table 2**, the closest values to this -3dB point is at +0.1° and -0.2°. The width of this band is exactly 0.3°. I The BWFN is observed to be at -0.6° and +0.7°. The first side lobes are also observed, occurring at -0.7° and +0.8°.

It is odd that these features are not centred at 0 however we also note that the Peak appears at a -0.1° elevation offset. These observations can be attributed to a combination of measurement error, and poor resolution.

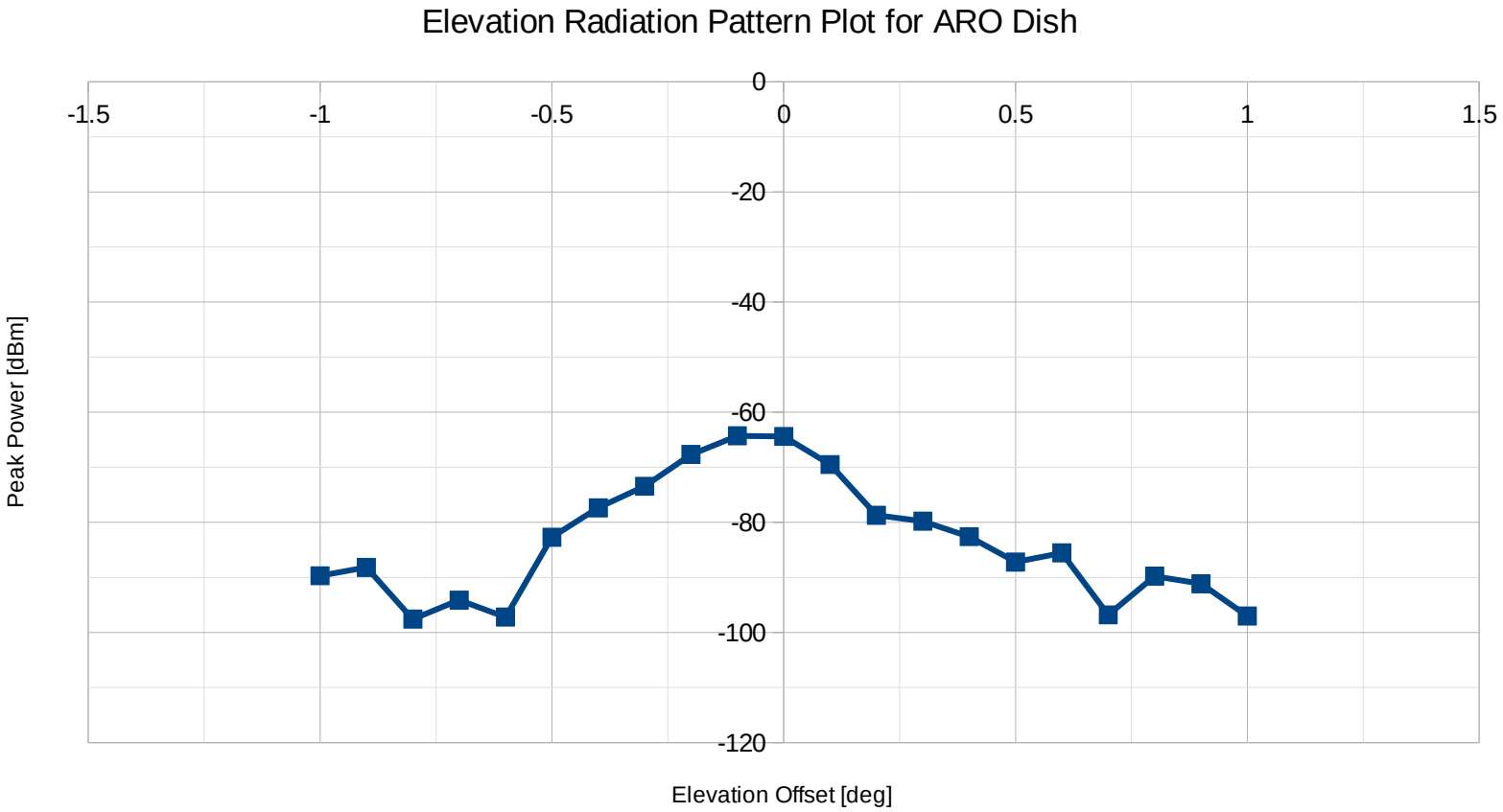

Figure 11: *Scatter plot of activity 1 measurements, peak power level over varying elevation angular displacement*

3.1.4 Azimuth Radiation Pattern

Although theoretically the peak power levels should occur at a 0° offset for both angles, the data obtained suggested a peak at -0.1° and so that was used for the azimuth measurement test. With a constant elevation offset of -0.1°, the measurements in **Table 3** were recorded. This data is presented as a plot in **Figure 12** below. This plot resembles an ideal pattern much better than the elevation plot, as it is much more symmetrical. I contribute this fact to "getting the hang of it", and a higher confidence in the accuracy of the recorded data. The peak power, -64.61 dBm, occurs at a 0° azimuth offset. The -3dB points would be around -67.61 dBm. The closest equivalents are at +-0.2°, thus giving a HPBW of 0.4°. The BWFN occur at +-0.6° . The first side lobes appear to be at +-0.7°. These results match very well with the elevation radiation pattern discussed previously.

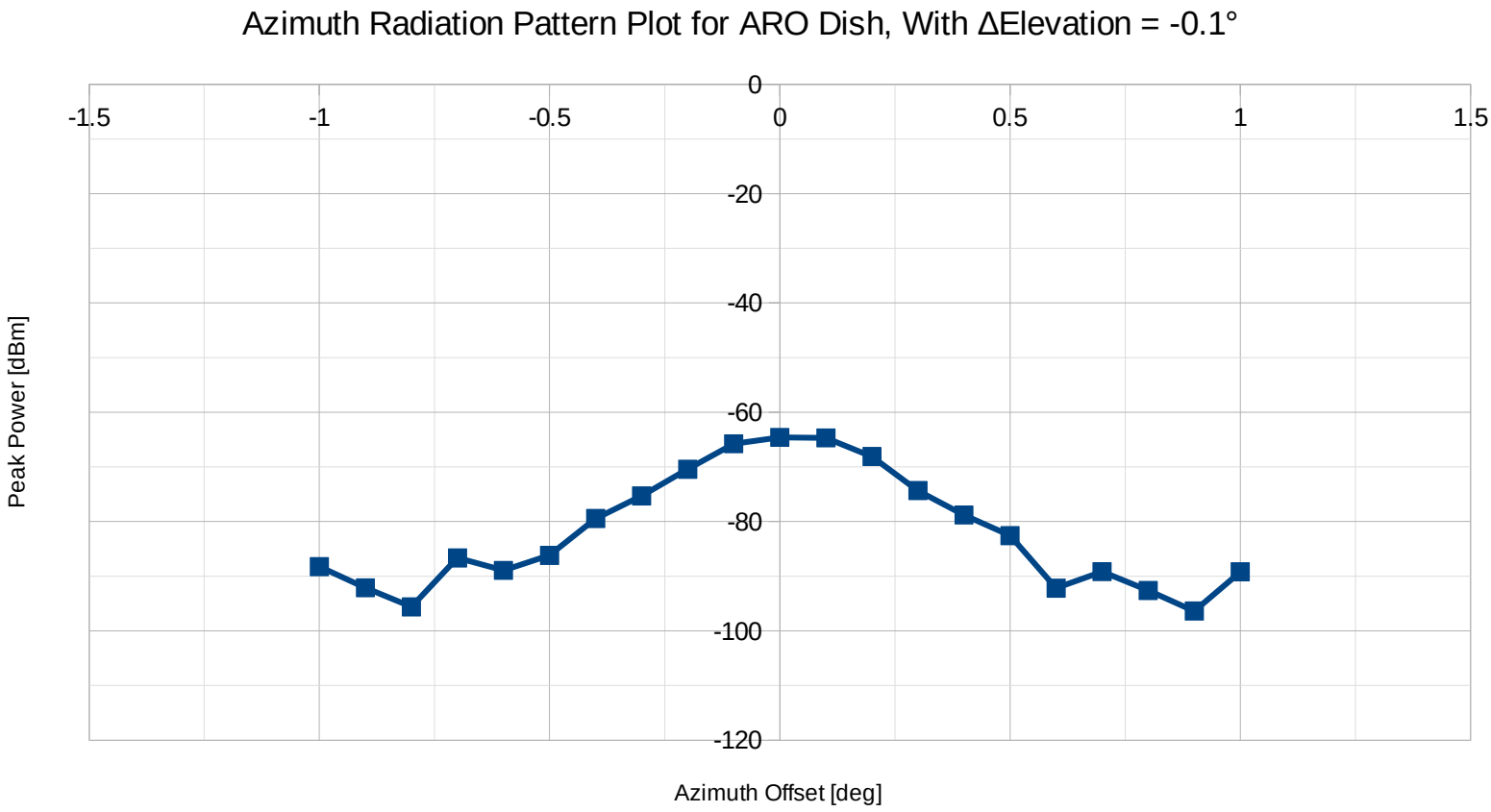

Figure 12: *Scatter plot of activity 1 measurements, peak power level over varying azimuth angular displacement*

3.1.5 System Gain

After measuring the radiation pattern for the ARO dish, the secondary purpose of this exercise was to compare the received power levels with our software package and determine the system gain. The link equation used by our program depends on EIRP, path loss, receive gain and system gain. The term "system gain" as used here is actually describing the atmospheric attenuation as well as any amplifier network used by ARO. Initially, the Gs value in the code was set to 0. When comparing the minimum power calculated with the actual power received during the exercise, it was found that our calculated power was about 4 dBm lower than it should be. So at this point, the code was altered so that Gs was 4 dBm. **Figure 13** illustrates the equation used and the Python function.

```python
def LinkBudget(R):
    R = R*10**3
    C = list()
    Ls = list()
    f = 1575.42e6 #Frequency Band Center, Hz
    eta = 0.5 #Antenna Efficiency
    D = 46 #Antenna Diameter m
    c = 3e8 #speed of light, m/s
    pi = np.pi
    Gr = np.log10((eta/c**2)*(pi*f*D)**2)*10 #recieve gain [dBW]
    Gs = 4 #TBD @ARO [dBW]
    EIRP = (26.1+26.8)/2 #placeholder value I got from a paper [dBW]
    for i in range(len(R)):
            Ls.append(np.log10((c/(4*pi*R[i]*f))**2)*10) #free space path loss [dBW]
            C.append( Ls[i] + Gr + Gs + EIRP + 30)
    return C
```

$$C = \overbrace{PL_1G_t}^{EIRP} \quad \overbrace{L_s}^{L_s=\left(\frac{c}{4\pi Rf}\right)^2} \quad \overbrace{G_r}^{G_r=\frac{\pi^2 f^2 D_r^2 \eta}{c^2}} \quad \overbrace{G_s}^{\text{System Gain}}$$

Figure 13: *Formula and code used to calculate the system linkage*

3.2 Activity 2, Spacecraft Tracking and Software Delivery

It should again be stated that the software package was in perfect working condition before travelling to ARO. Many hours were spent testing and debugging the code before the trip to get to that point. All the access times, look angles, and ranges were verified through STK. The only factor that remained to be determined was the pointing file itself.

According to the software specification document, it was legal to have multiple comment lines (prefaced with a #). So the pointing file output function used this as an opportunity to describe the simulation parameters in detail (i.e date, time, satellite, etc). However, after talking with the technician, it was discovered that there could only actually be one comment line at the beginning of the code. So the code was quickly modified to accommodate for that. With that fix in place, as well as with the updated link budget, the software package was ready for testing.

During the experiment, the package performed very well. It ran quite efficiently, operating for a half hour tracking interval and 5 second time step, for 31 satellites, in about 35 seconds. The ARO system accepted the pointing file with no problems, and the a signal was observed on the spectrum analyzer. Comparing the results of the developed code (**Figure 5**), with the results of a professional tracking software (**Figure 1**), we see that under the same spectrum analyzer settings the two plots are very similar. We see the centre frequency occur at 1.575 GHz, which is exactly as we expect for an L-band transmission. We also see a power level similar to what the software predicted.

3.3 Activity 3, Mystery TLE

The spectrum observed during this activity (**Figure 7**) was for an unknown satellite. Referring to chart in **Figure 14**, we see the four kinds of global positioning satellites, BEIDOU, GPS, GALILEO, and GLONASS, as well as their designated bands. The frequencies marked along the abscissa indicate the centre frequencies for the upper/lower portion of the L band. Comparing the frequency spectrum obtained with this chart, it was quickly observed that there were two distinct groupings of peaks. The positions of these peaks corresponded to the E6, and B1/E1/L1 locations.

Based on this observation, the mystery satellite was narrowed down to either BEIDOU or GALILEO. The team had a discussion about how to determine which one it was. There was some initial confusion because of the upper cluster, as it appeared not to fit into either B1 or E1. However by adjusting the spectrum analyzer to get very precise measurements, it was found that the lower centre frequency occurred at 1.2686 GHz , and the upper centre frequency was approximately 1.5686 GHz. This gave us enough evidence to identify the satellite as a BEIDOU type.

This train of thought was successful, as the technician confirmed that we were in fact tracking BEIDOU-3.

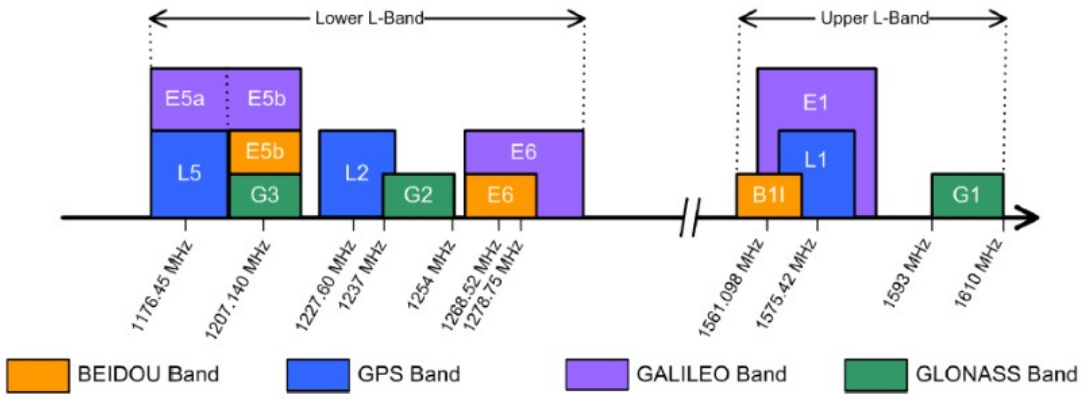

4.0 Conclusion

The purpose of these activities was to apply all of the core concepts of the course to a practical space engineering scenario. Going into the field gave me a real world understanding of RF communications beyond the classroom lectures, and helped me realize practicality of why we learned these concepts. In particular, concepts like a dish radiation pattern that we explored in previous labs suddenly clicked for me, and I feel like I have a much better intuition for RF theory now.

Developing the software package was a difficult task, but it greatly improved my programming abilities. I learned practical engineering concepts like project management, working with a team, product testing, and debugging. All of the problems faced during development reinforced my understanding of fundamental concepts, like transformation between coordinate systems, orbital parameters and TLE, astronomy and look angles. Utilizing STK for testing also gave me an opportunity to sharpen my skills with a professional software.

All of the weekly milestones during development (P1, P2...) were successfully accomplished on time. Feedback on the reports were considered and used to improve on each subsequent phase. The software was fully tested, debugged, and operational end to end before travelling to ARO. The code ran efficiently, the pointing file was able to point the dish, the computed look angles were on target, and all activities were accomplished successfully. The results from each activity fit our hypotheses, and all observations fit with our understanding of analog, digital, and RF theory.

5.0 References

[1] **"***Antenna Theory - Beam Width"*

https://www.tutorialspoint.com/antenna_theory/antenna_theory_beam_width.htm

[2] "*T7*" - Hugh Chesser, PHYS4350 Lecture Material, York University 2018